Hindawi
Advances in Materials Science and Engineering
Volume 2022, Article ID 9144673, 9 pages
https://doi.org/10.1155/2022/9144673

Research Article

Strength Characteristics and Failure Mechanism of Granite with Cross Cracks at Different Angles Based on DIC Method

Xu Wu,[1] **Liyuan Zhang**,[2] **Jinglai Sun**,[1] **Qifeng Guo**,[3] **Jiliang Pan**,[3] **and Jun Gao**[1]

[1]*Beijing Municipal Engineering Research Institute, Beijing 100037, China*
[2]*CNBM Geological Engineering Exploration Academy Co. Ltd, Beijing 100102, China*
[3]*School of Civil and Resource Engineering, University of Science and Technology Beijing, Beijing 100083, China*

Correspondence should be addressed to Qifeng Guo; guoqifeng@ustb.edu.cn

Received 2 January 2022; Revised 12 February 2022; Accepted 21 February 2022; Published 16 March 2022

Academic Editor: REN Fuqiang

The engineering rock mass is generally composed of the rock matrix and structural plane and is an anisotropic inhomogeneous geological body. Accidents such as roof collapse and well caving caused by joint and fissure expansion occur frequently during tunnel excavation and service, resulting in serious casualties and economic losses. It is of great theoretical significance and engineering value to study the fracture mechanism of the jointed rock mass to ensure the stability of the surrounding rock and the safe and efficient utilization of the urban underground space. To investigate the effects of crossed cracks on mechanical properties and failure characteristics of rock, wire cutting equipment is employed to make rock samples with different crossed cracks, and then acoustic emission system and digital image correlation technique are used to study the fracture process of rock samples under uniaxial compression. It has been found that the strength of rock samples with a single crack is generally larger than that of samples with cross cracks, and the strength changed with the angle of the crack in a "V" shape. When the angle of preexisting crack is 60°, the rock strength reaches the lowest. The primary crack has a more obvious influence on rock strength and is the main controlling factor of rock fracture. The initiation stress of rock samples with a single crack changes more significantly with angle. When the angle of the primary crack is 45°, the rock sample is most prone to crack initiation failure, and the crack initiation stress is only 1/4 to 1/2 of the strength. There are two types of cracks: wing and anti-wing, and the tensile cracks are the main ones. It is revealed that the fracture of cracked rock has significant directional characteristics. For the samples with cross cracks, the primary crack is the main control factor of crack initiation, and the secondary crack has a certain guiding effect on the crack.

1. Introduction

Rock mass in nature is a heterogeneous and discontinuous multiphase composite material, which contains a large number of natural defects. Under the action of external loads, these preexisting joints or fissures will expand and connect with each other, thus forming macrocracks, resulting in rock mass failure. A large number of studies show that the geometry of joints (e.g., angle, width, length, quantity, and so on) has an important effect on the strength and deformation behavior of jointed rock masses. For example, Lajtai [1–3] studied the initiation law of preexisting cracks under external loading by using rock-like materials and summarized the types and propagation modes of new cracks in detail. Chen et al. [4–6] conducted uniaxial compression tests on samples made of gypsum and studied the influence of factors such as joint spacing, dip angle, and connectivity on the strength, elastic modulus, and stress-strain relationship of a discontinuous jointed rock mass. Liu et al. [7] systematically analyzed the peak strength and failure mode of preexisting jointed rock mass under uniaxial compression under seven working conditions, including different joint dip angles, joint coherence, and number of joint groups. Wang et al. [8] studied the combined effect of joint density and dip angle on the strength and deformation characteristics of the sample with open joints under uniaxial compression. Guo et al. [9, 10] used water jet cutter technology to prepare real granite cracked samples and analyzed the crack initiation law, strength characteristics, and failure mode of the cracked rock mass under uniaxial compression.

Furthermore, Shen et al. [11] conducted uniaxial compression tests on a series of cracked gypsum samples, analyzed the coalescing and fracture mechanisms of the rock bridge, and found that they were related to the relative positions of two parallel cracks. Zhou et al. [12] conducted an experimental study on rock samples with cross cracks, which demonstrated the generation, expansion, and merger process of two three-dimensional cracks in rock-like samples under uniaxial compression. Zhang et al. [13, 14] conducted uniaxial compression tests on 20 groups of rock samples containing cross cracks, studied the influence of the angle between primary and secondary cracks on the failure mode and mechanical properties of the rock samples, and explored the failure mechanism of the cross-cracked rock mass with Abaqus numerical software. With the aid of acoustic emission technology and a surface strain measurement system, Xu et al. [15] prefabricated orthogonal cross cracks with different distribution states with wire cutting equipment and analyzed the crack initiation stress, propagation path, and stress properties of granite samples under uniaxial compression. Chen et al. [16] studied the uniaxial compression mechanical properties and deformation law of the "T" shaped cross-cracked rock samples, and the study showed that the main crack dip angle played a decisive role in the peak stress of the sample, while the secondary crack affected the peak stress of the sample to a certain extent. Based on DIC and AE techniques, Pan et al. [17] studied the prefailure energy evolution of granite with conjugate joints in uniaxial compression tests.

Cross cracks widely exist in the actual rock mass. The laboratory study on the mechanical fracture evolution of samples with cross cracks at different angles can provide important guidance for rock mass engineering [18–20]. Although a large number of studies have been carried out on the mechanical properties and damage evolution of prefabricated rock samples with fractures, there are few studies on the mechanical characteristics of rock samples with fractures, and most of them are confined to the description and qualitative interpretation of experimental phenomena [21–23]. At present, the study of cross cracks in natural rocks is a research focus in the field of rock fracture mechanics [24–26]. In this paper, uniaxial compression experiments of granite samples with cross cracks were performed using the compression-testing machine system and the AE testing system. At the same time, the DIC system was used to study the evolution of the local stress field at different loading times. Based on physical tests, this paper will explore the strength characteristics and crack propagation law of cross-cracked granite samples, reveal their fracture mechanism, and provide theoretical guidance for the stability prediction of fractured rock mass and the deformation control of underground space engineering structure.

2. Cracked Samples and Testing Methods

The matrix of granite contains fine grains, and the granite with an average porosity of 1.29% is composed of quartz, potassium feldspar, and biotite. The average density of the samples is 2.6 g/cm^3, and the P-wave velocity is about 4950 m/s. In order to facilitate the monitoring of the crack propagation path during the loading test, the granite samples are machined to be cube with 50 mm length, 25 mm width, and 100 mm height. As illustrated in Figure 1, the central position of the sample is prefabricated with a size of 20 mm × 0.3 mm (primary crack) and 15 mm × 0.3 mm (secondary crack) through cracks. The primary crack and secondary crack are indicated by red line and blue line, respectively. The angle between the primary crack and the secondary crack is α, and the included angle between the primary crack and the vertical direction of the specimen is β. In the experiment, five included angle changes of 0°, 30°, 45°, 60°, and 90° were considered, so there are 25 distribution states of cross joints. The typical samples with cross cracks are shown in Figure 2.

Uniaxial compression tests are carried out on the GAW-2000 rigid testing machine as shown in Figure 3. The loading is controlled by the apparatus displacement with a speed of 0.03 mm/min. During the loading process, acoustic emission monitoring and digital image correlation technique are used to collect the acoustic emission data and surface strain data at intervals of 0.5 s and 1 s, respectively.

3. Test Results

3.1. Strength and AE Characteristics. The stress and AE events of the samples along the loading time are obtained in Figure 4. It can be found that with the loading time increasing, the stress of the sample gradually increases to the compression strength and then decreases suddenly because of failure. During the uniaxial compression test, there are almost no acoustic emission events in the crack compaction stage and elastic stage. Only when the crack initiation stage is reached, the acoustic emission count will increase suddenly. Therefore, we take the stress when the AE counts suddenly increase as the crack initiation stress. After rock initiation, AE events continue to occur, and cracks continue to develop and expand until rock failure. As shown in Figure 4, AE events occur at different time points due to the preexisting cracks, and the initiation stress of the rock also varies greatly with the preexisting cracks. The uniaxial compression strengths (i.e., UCS) and crack initiation stresses (i.e., CIS) of the samples with different cracks are shown in Table 1.

According to the data analysis in Table 1, the uniaxial compression strength and initiation stress of the cracked samples are lower than those of the samples without the crack. When the angles of β and α are 0° (i.e., the crack is parallel to the loading direction), the average value of uniaxial compression strength is 115.65 MPa and the average value of crack initiation stress is 88.27 MPa, which are the largest in the samples. On the contrary, the compressive strength and initiation stress of rock samples are the lowest when $\beta = 60°$ and $\alpha = 60°$. The variation in crack initiation stress with crack angle is shown in Figure 5.

As shown in Figure 5(a), when the angle of β is 0°, the initiation stress of the rock samples decreases gradually with the increase of α, when the two cracks are orthogonal, the initiation stress is the lowest, and the initiation stress of the crack has an obvious response to the variation of crack angle.

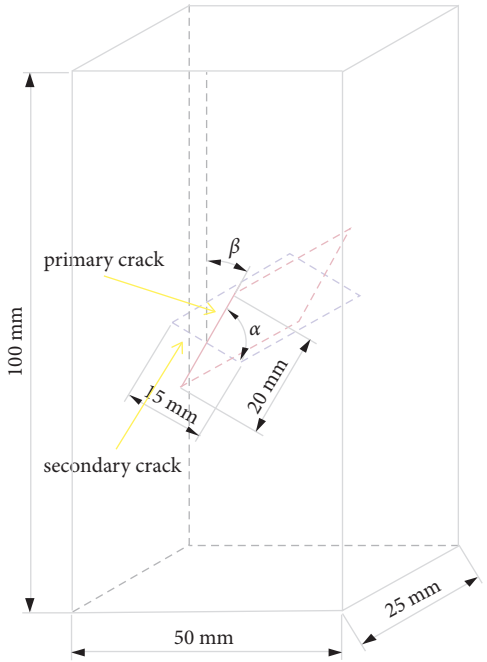

Figure 1: Illustration of the granite sample with crossed cracks.

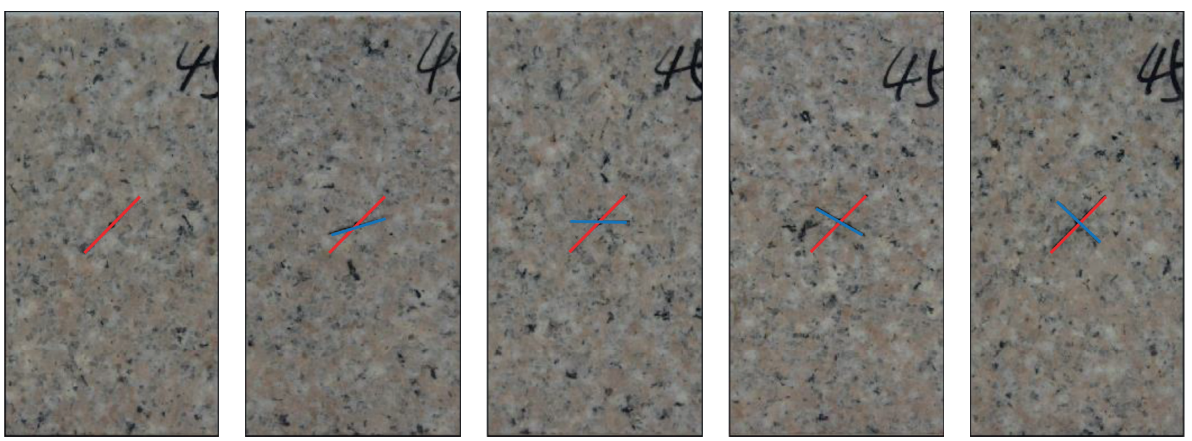

Figure 2: Cross-cracked samples: (a) $\alpha = 45^\circ$, $\beta = 0^\circ$; (b) $\alpha = 45^\circ$, $\beta = 30^\circ$; (c) $\alpha = 45^\circ$, $\beta = 45^\circ$; (d) $\alpha = 45^\circ$, $\beta = 60^\circ$; (e) $\alpha = 45^\circ$, $\beta = 90^\circ$.

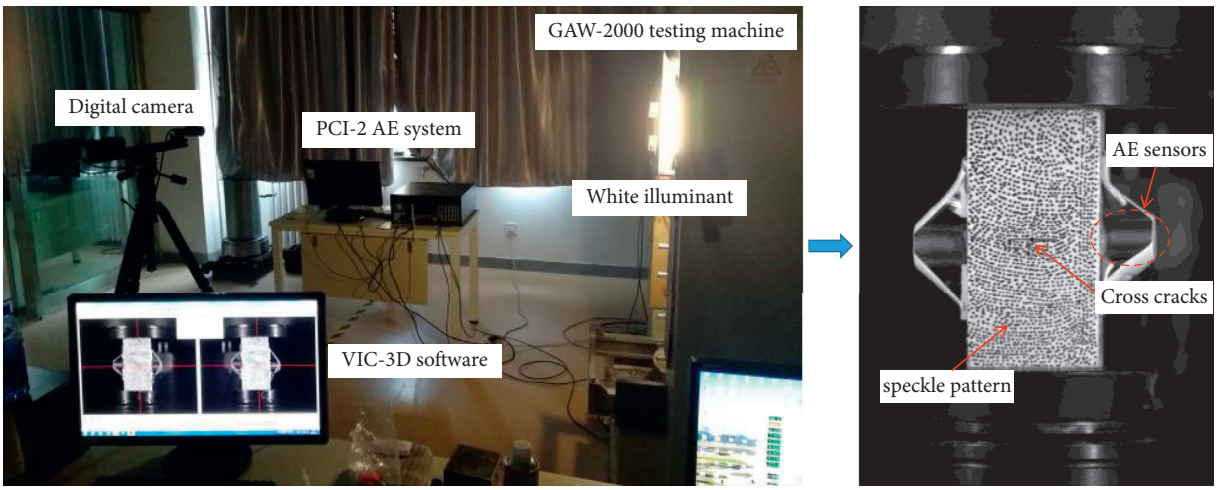

Figure 3: Testing system.

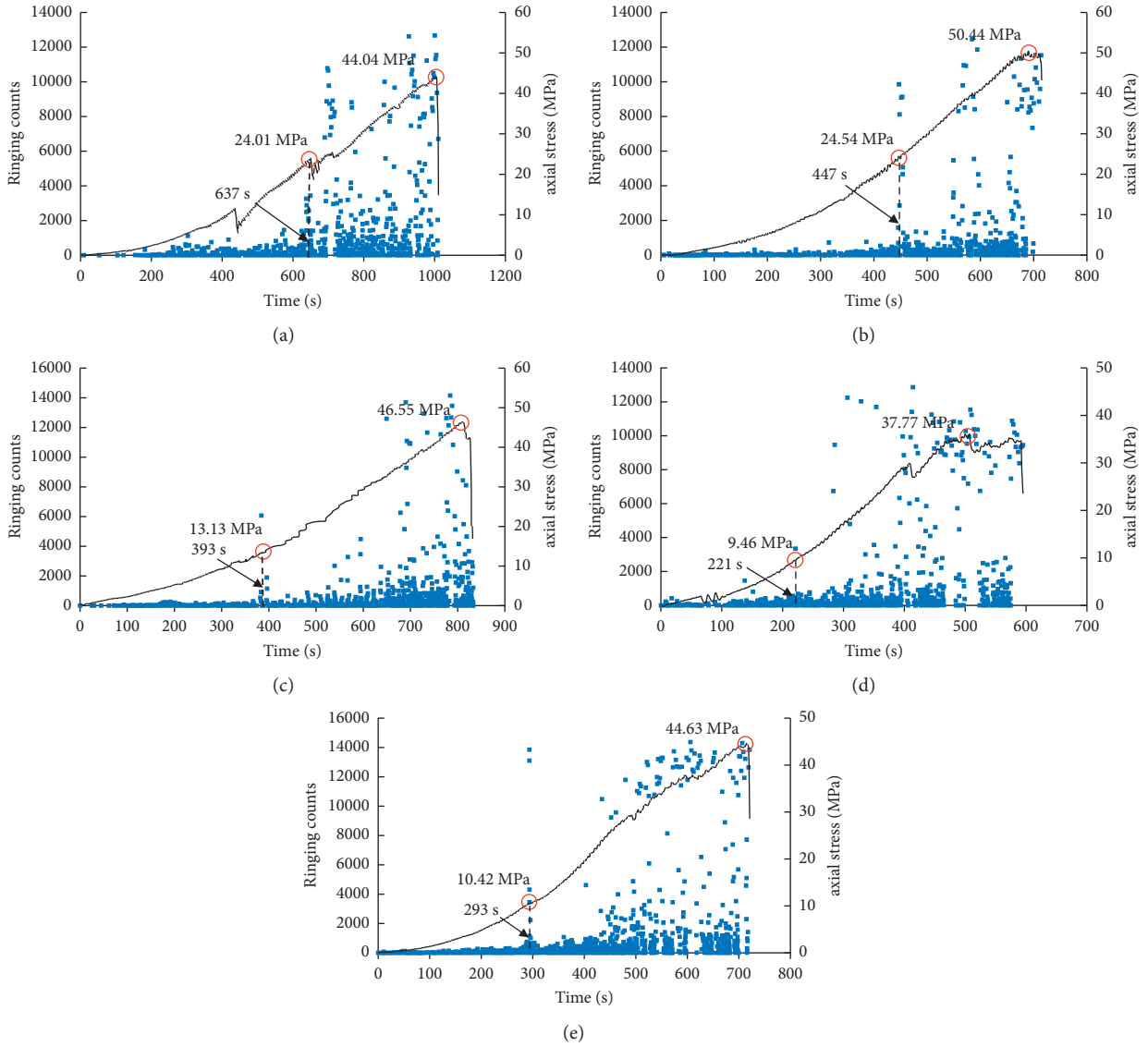

Figure 4: Acoustic emission ringing count-time-axial stress diagram: (a) $\alpha = 45^{\circ}$, $\beta = 0^{\circ}$; (b) $\alpha = 45^{\circ}$, $\beta = 30^{\circ}$; (c) $\alpha = 45^{\circ}$, $\beta = 45^{\circ}$; (d) $\alpha = 45^{\circ}$, $\beta = 60^{\circ}$; (e) $\alpha = 45^{\circ}$, $\beta = 90^{\circ}$.

When $\beta > 0^{\circ}$, the crack initiation stress varies less; however, according to the analysis of the overall variation law, the crack initiation stress of rock samples decreases first and then increases with the angle between cracks, and the crack initiation stress is generally minimum when α is 45° or 60°. Therefore, the smaller α, the higher the initiation stress of the rock. When the crack angle α is constant, the crack initiation stress of rock samples decreases first and then increases with the increase of the main crack angle β, as shown in Figure 5(b), the minimum initiation stress occurs when β is 45° or 60°, and the response of single crack to rock initiation stress is more significant.

The ratio of crack initiation stress to peak strength is defined as the crack initiation stress ratio η, $\eta = \sigma_i/\sigma_c$, where σ_i is the initiation stress of rock and σ_c is the peak strength of rock. According to the distribution range of η in Figure 6, the initiation stress of rock samples is 20% to 80% of the peak strength. The crack initiation stress ratio of rock samples with a single crack is generally larger than that of rock samples with cross cracks. When the angles of a single crack are 0° or 90°, η reaches 0.76 and 0.77, respectively. At this point, the sample exhibits a strong and rapid brittle failure, and the rapid development of cracks at the end of the crack leads to the overall failure of the sample. At the same time, the rock samples with higher initiation stress have more energy gathering before crack initiation and faster energy release rate after initiation.

When the crack angle α is constant, the crack initiation stress ratio η decreases firstly and then increases with the increase of β. When β is 45°, the rock sample is more prone to crack initiation, and the crack initiation stress is only 1/4 to 1/2 of the peak strength. Such rock samples are fractured under the action of lower load, and the energy gathered in the initial stage is released, the failure of rock samples is

Table 1: UCS and CIS of the samples with different crack angles.

Sample number	Uniaxial compression strength (i.e., UCS) (MPa)	Crack initiation stress (i.e., CIS) (MPa)	The stress ratio (between CIS and UCS)
00-00	115.65	88.27	0.76
00-30	97.85	46.98	0.48
00-45	52.43	33.49	0.64
00-60	57.61	23.07	0.40
00-90	47.91	19.28	0.40
30-00	80.76	29.38	0.36
30-30	64.44	29.60	0.46
30-45	59.35	24.49	0.41
30-60	62.91	25.94	0.41
30-90	62.12	26.31	0.42
45-00	44.04	24.01	0.55
45-30	50.44	24.54	0.49
45-45	46.55	13.13	0.28
45-60	37.77	9.46	0.25
45-90	44.63	10.42	0.23
60-00	38.26	17.22	0.45
60-30	40.55	16.20	0.40
60-45	43.74	21.35	0.49
60-60	25.23	9.08	0.36
60-90	41.64	24.32	0.58
90-00	43.14	33.33	0.77
90-30	40.94	18.03	0.44
90-45	42.45	14.99	0.35
90-60	46.33	23.88	0.52
90-90	36.94	23.20	0.63

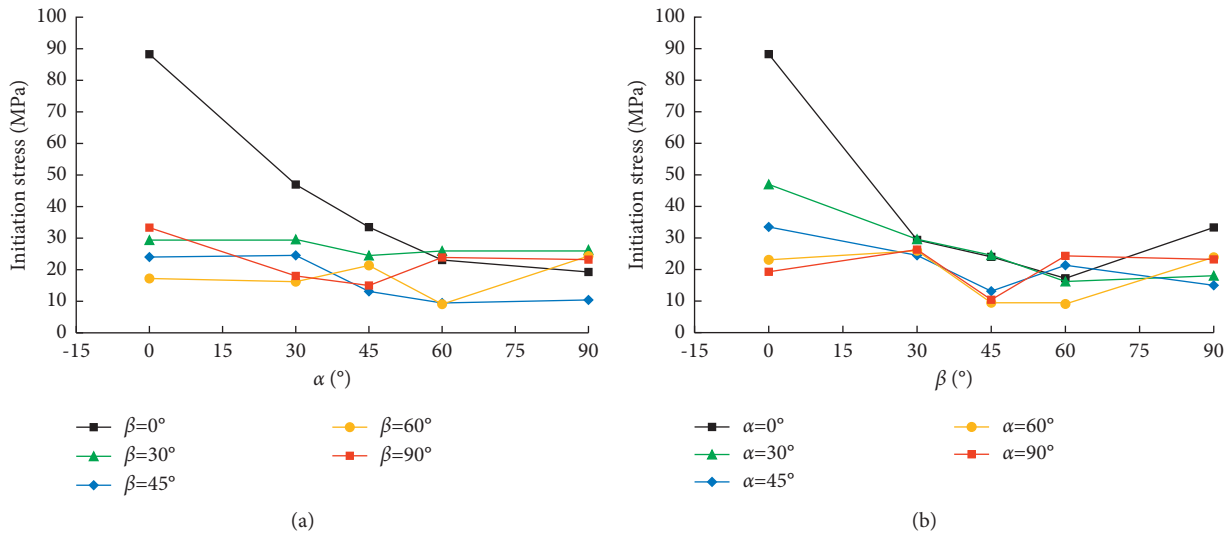

Figure 5: Variation law of crack initiation stress of rock with crossed cracks. (a) Relationship between crack initiation stress and α. (b) Relationship between crack initiation stress and β.

progressive, and the crack growth rate is relatively slow. On the contrary, when β is 0° or 90°, the crack stress ratio is higher. The failure process of two samples is relatively quick and shows a more obvious brittle failure characteristic. There is no obvious warning before rock failure, so it is difficult to prevent and predict such rock failure. According to the analysis of the initiation stress and the stress ratio η, when β is 45° or 60°, not only the initiation stress is low but also the fracture is easy to occur, and the crack has a great influence on the initiation characteristics of rock samples.

3.2. Surface Maximum Principal Strain Characteristics. There are usually two kinds of cracks at the preexisting crack end of rock material: wing cracks and secondary cracks. Most scholars believe that rock is dominated by wing

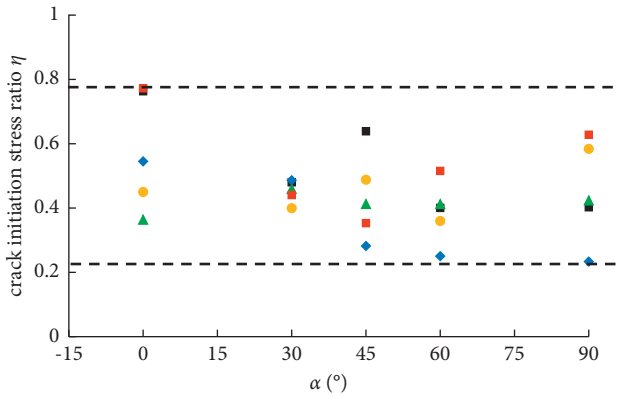

Figure 6: Distribution diagram of crack initiation stress ratio η.

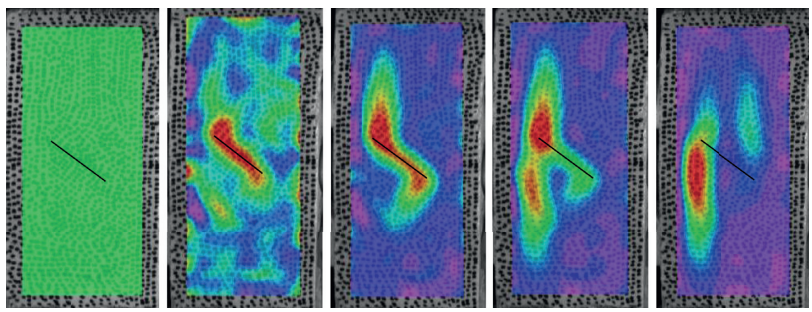

(a)

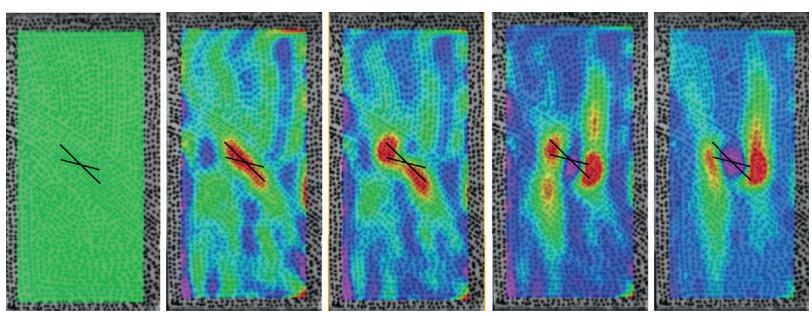

(b)

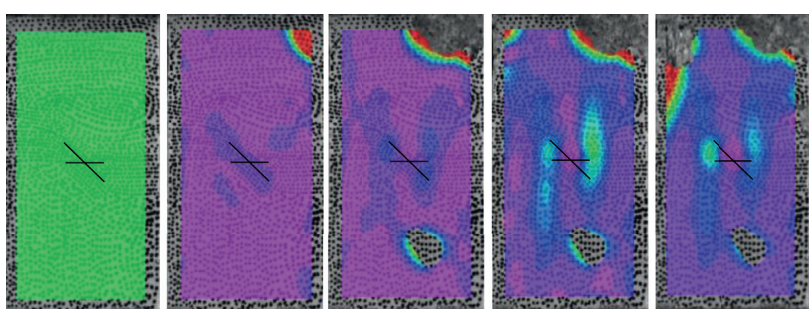

(c)

Figure 7: Continued.

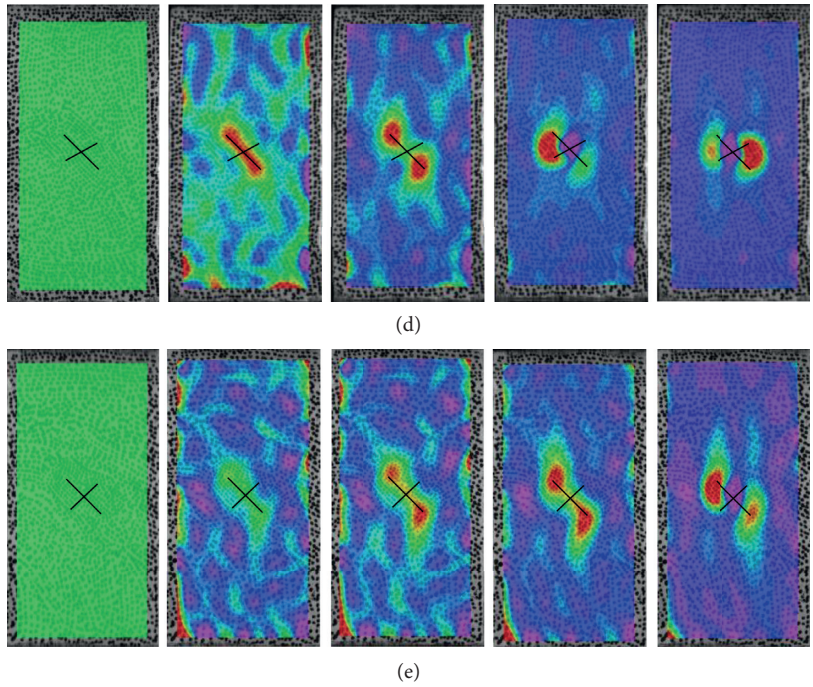

Figure 7: Surface maximum principal strain characteristics of the samples with different cross cracks: (a) $\alpha = 45^\circ$, $\beta = 0^\circ$; (b) $\alpha = 45^\circ$, $\beta = 30^\circ$; (c) $\alpha = 45^\circ$, $\beta = 45^\circ$; (d) $\alpha = 45^\circ$, $\beta = 60^\circ$; (e) $\alpha = 45^\circ$, $\beta = 90^\circ$.

initiation, and wing cracks under tensile stress start at the preexisting crack end and propagate along the direction of maximum load. However, the fracture of cracked rock is different from initiation, and a large number of tests show that the secondary crack caused by shear stress or compound stress is the main factor leading to the failure of samples. The final failure modes of rock with cross cracks are analyzed by using surface strain data, and the stress types and crack propagation characteristics leading to rock failure are discussed. The variation in surface deformation characteristics with crack propagation is shown in Figure 7.

Compared to the crack distribution characteristics of intact rock samples, the 00-00 sample presents a compression shear failure, forming a fracture zone with an angle of 27° with the loading direction. The failure of other rock samples with single cracks and cross cracks starts from the preexisting crack tip, generating wing or anti-wing cracks and expanding along the loading direction, resulting in the instability failure of the sample. Crack distribution patterns control and guide the initiation and failure of rocks. As the axial stress increases, the wing or anti-wing cracking occurs mainly at the crack end of rock under the action of tensile stress. According to the time of fracture and the analysis of the variation characteristics of the strain field on the rock surface shown in Figure 7, the fracture of the rock with cross cracks is mainly controlled by the primary crack and the secondary crack has a certain guiding effect on the propagation of the crack.

For the sample whose primary crack is perpendicular to the loading direction, an oval stress concentration zone appears in the middle of the crack at the initial loading stage. As shown in Figure 7, with the increase of axial stress, the stress concentration zone shifts from the vicinity of the secondary crack to the tip of the primary crack, and the crack initiation is approximately parallel to the loading direction. Therefore, when there is a crack orthogonal to the loading direction in the rock sample, this crack controls the new crack initiation and failure of the rock. The crack initiation is concentrated at the end of the preexisting crack and extends to both ends of the sample in a form approximately parallel to the loading direction. According to the initiation position, when the included angle between the secondary crack and the vertical direction of the specimen is small, the crack initiation is located at the upper or lower part of the preexisting crack and cracks in one side direction. When the included angle between the secondary crack and the vertical direction of the specimen is greater than 45°, the initiation crack is concentrated and symmetrically distributed at the midpoint of the primary crack.

4. Conclusions

An experimental approach on the crack initiation mechanism in granite samples under uniaxial compression was carried out. Some conclusions could be drawn as follows.

The uniaxial compression test of rock with cross cracks was carried out, and the variation law of peak strength and crack initiation stress of granite with cross cracks was obtained. It was found that the strength of rock with a single crack is generally larger than that of rock with cross cracks, and the strength of the sample changed with the angle of crack in a "V" shape. When the angle of preexisting crack is 60°, the rock strength reaches the lowest. The primary crack

has more obvious influence on rock strength and is the main controlling factor of rock fracture.

Acoustic emission monitoring tests were carried out to determine the crack initiation stress by acoustic emission ringing counting, and the variation law of crack initiation stress at crack end was obtained. When the crack angle is constant, the crack initiation stress decreases first and then increases with the increase of the primary crack angle. The crack initiation stress of rock samples with a single crack changes more significantly with angle. The ratio of crack initiation stress to peak strength is taken as an index to judge the degree of rock failure. When the inclination angle of the primary crack is 45°, the rock sample is most prone to crack initiation failure, and the crack initiation stress is only 1/4 to 1/2 of the peak strength.

By means of the non-contact surface strain field (DIC) device, the law of crack initiation and the distribution pattern of cracks in rock samples with intersecting fractures are studied. Cracks are found to be mainly wing or anti-wing, and the tensile cracks are the main ones. It is revealed that fracture of cracked rock has significant directional characteristics. For the samples with cross cracks, the primary crack is the main control factor for crack initiation, and the secondary crack has a certain guiding effect on the crack.

It is an important means to control the crack initiation in underground tunnel engineering to prevent side falling and roof-fall accidents. According to the crack initiation mechanism and the variation characteristics of the crack initiation stress and the maximum strength, the accurate support scheme for the fractured rock mass as well as the key construction part and the time node of the protection project can be established by combining the magnitude of the pressure and direction of the slope or the underground engineering.

Data Availability

The experimental data used to support the findings of this study are included within the article.

Conflicts of Interest

The authors declare that there are no conflicts of interest regarding the publication of this paper.

Acknowledgments

This research was funded by the Beijing Municipal Natural Science Foundation (grant no. 8214049).

References

[1] E. Z. Lajtai, "Brittle fracture in compression," *International Journal of Fracture*, vol. 10, no. 4, pp. 525–536, 1974.

[2] A. Bobet and H. H. Einstein, "Fracture coalescence in rock-type materials under uniaxial and biaxial compression," *International Journal of Rock Mechanics and Mining Sciences*, vol. 35, no. 7, pp. 863–888, 1998.

[3] M. Sagong and A. Bobet, "Coalescence of multiple flaws in a rock-model material in uniaxial compression," *International Journal of Rock Mechanics and Mining Sciences*, vol. 39, no. 2, pp. 229–241, 2002.

[4] X. Chen, J. Sun, P. Yang, and Z. Feng, "Influence of joint spacing and inclination angle on fragmentation characteristic of rock masses under uniaxial compression," *Journal of Mining & Safety Engineering*, vol. 34, no. 3, pp. 608–614, 2017, in Chinese.

[5] X. Chen, D. Li, and L. Wang, "Experimental study on effect of spacing and inclination angle of joints on strength and deformation properties of rock masses under uniaxial compression," *Chinese Journal of Geotechnical Engineering*, vol. 36, no. 12, pp. 2236–2245, 2014, in Chinese.

[6] X. Chen, Z. Liao, and D. Li, "Experimental study of effects of joint inclination angle and connectivity rate on strength and deformation properties of rock masses under uniaxial compression," *Chinese Journal of Rock Mechanics and Engineering*, vol. 30, no. 4, pp. 781–789, 2011, in Chinese.

[7] H. Liu, Y. Huang, and K. Li, "Test study of strength and failure mode of pre-existing jointed rock mass," *Rock and Soil Mechanics*, vol. 34, no. 5, pp. 1235–1241, 2013, in Chinese.

[8] P. Wang, P. Cao, and C. Pu, "Effect of the density and inclination of joints on the strength and deformation properties of rock-like specimens under uniaxial compression," *Chinese Journal of Engineering*, vol. 39, no. 4, pp. 494–501, 2017, in Chinese.

[9] Q. Guo, W. U. Xu, and M. Cai, "Experiment on the strength characteristics and failure modes of granite with pre-existing cracks," *Chinese Journal of Engineering*, vol. 41, no. 01, pp. 43–52, 2019, in Chinese.

[10] Q. Guo, W. U. Xu, and M. Cai, "Crack initiation mechanism of pre-existing cracked granite," *Journal of China Coal Society*, vol. 44, no. S2, pp. 476–483, 2019, in Chinese.

[11] B. Shen, O. Stephansson, H. H. Einstein, and B. Ghahreman, "Coalescence of fractures under shear stresses in experiments," *Journal of Geophysical Research: Solid Earth*, vol. 100, no. B4, pp. 5975–5990, 1995.

[12] X.-P. Zhou, J.-Z. Zhang, and L. N. Y Wong, "Experimental study on the growth, coalescence and wrapping behaviors of 3D cross-embedded flaws under uniaxial compression," *Rock Mechanics and Rock Engineering*, vol. 51, no. 5, pp. 1379–1400, 2018.

[13] Bo Zhang, S. Li, and X. Yang, "Uniaxial compression failure mechanism of jointed rock mass with cross-cracks," *Rock and Soil Mechanics*, vol. 35, no. 7, pp. 1863–1870, 2014, in Chinese.

[14] Bo Zhang, S. Li, and X. Yang, "Uniaxial compression tests on mechanical properties of rock mass similar material with cross-cracks," *Rock and Soil Mechanics*, vol. 33, no. 12, pp. 3674–3679, 2012, in Chinese.

[15] W. U. Xu, F. Wang, and X. I. Xun, "Experimental investigation on the strength characteristics and fracture mechanism of rock with orthogonally crossed cracks," *Journal of China Coal Society*, vol. 45, no. 7, pp. 2681–2690, 2020, in Chinese.

[16] Y. Chen, P. U. Cheng, and G. Li, "Experimental study on mechanical properties of rock mass samples with T-shaped cross crack subjected to uniaxial compression," *Journal of Experimental Mechanics*, vol. 34, no. 4, pp. 684–692, 2019, in Chinese.

[17] J. Pan, X. Wu, Q. Guo, and X. Xi, "Uniaxial experimental study of the deformation behavior and energy evolution of conjugate jointed rock based on AE and DIC methods," *Advances in Civil Engineering*, vol. 2020, Article ID 8850250, 16 pages, 2020.

[18] J. Pan, F. Ren, and M. Cai, "Effect of joint density on rockburst proneness of the elastic-brittle-plastic rock mass," *Shock and Vibration*, vol. 2021, Article ID 5574325, 9 pages, 2021.

[19] J. Sun, F. Wang, Z. Li, and D. Ren, "A new hybrid copula-based nonparametric Bayesian model for risk assessments of water inrush," *Quality and Reliability Engineering International*, p. 20, 2022.

[20] C. Zhu, M. C. He, X. H. Zhang, Z. G. Tao, Q. Yin, and L. F. Li, "Nonlinear mechanical model of constant resistance and large deformation bolt and influence parameters analysis of constant resistance behavior," *Rock and Soil Mechanics*, vol. 42, no. 7, pp. 1911–1924, 2021.

[21] C. Zhu, M. C. He, B. Jiang, X. Z. Qin, Q. Yin, and Y. Zhou, "Numerical investigation on the fatigue failure characteristics of water-bearing sandstone under cyclic loading," *Journal of Mountain Science*, vol. 18, no. 12, pp. 3348–3365, 2021.

[22] G. Li, Y. Hu, S. M. Tian, M. Weibin, and H. L. Huang, "Analysis of deformation control mechanism of prestressed anchor on jointed soft rock in large cross-section tunnel," *Bulletin of Engineering Geology and the Environment*, vol. 80, no. 12, pp. 9089–9103, 2021.

[23] M. Z. Gao, J. Xie, Y. N. Gao et al., "Mechanical behavior of coal under different mining rates: a case study from laboratory experiments to field testing," *International Journal of Mining Science and Technology*, vol. 31, no. 5, pp. 825–841, 2021.

[24] M. Z. Gao, H. C. Hao, S. N. Xue et al., "Discing behavior and mechanism of cores extracted from Songke-2 well at depths below 4,500 m," *International Journal of Rock Mechanics and Mining Sciences*, vol. 149, Article ID 104976, 2022.

[25] C. Cao, W. Zhang, J. P. Chen, B. Shan, S. Y. Song, and J. W. Zhan, "Quantitative estimation of debris flow source materials by integrating multi-source data: a case study," *Engineering Geology*, vol. 291, Article ID 106222, 2021.

[26] Z. Dou, S. X. Tang, X. Y. Zhang et al., "Influence of shear displacement on fluid flow and solute transport in a 3D rough fracture," *Lithosphere*, vol. 2021, Article ID 1569736, 2021.